

Dynamic response and fluid structure interaction of submerged floating tunnels

S. Remseth¹, B. J. Leira², A. Rönquist¹ & G. Udahl¹

¹*Department of Structural Engineering,*

Norwegian University of Science and Technology, Norway

²*Department of Marine Technology,*

Norwegian University of Science and Technology, Norway

Abstract

Stochastic dynamic response analyses are applied to study the behaviour of submerged floating tunnels subjected to wave loading. The earthquake response of a submerged tunnel with a tether mooring is studied by finite element modelling of the bridge and surrounding fluid. The numerical examples with wave loading emphasize effects of wave direction and shortcrestedness. The focus is on the need for integrated versus simplified modelling in earthquake response analysis.

Keywords: submerged floating tunnels, stochastic dynamic analysis, wave load modelling, wave directionality, time domain earthquake analysis, finite element modelling, dynamic fluid structure interaction.

1 Introduction

The submerged floating tunnel in Fig 1 is proposed to cross a Norwegian fjord with a maximum depth of 150 meters and a crossing distance of 1500 meters. The position of the tunnel relative to the surface is in this concept defined by mooring with tethers to the bottom at four positions along the bridge. Alternatively the tunnel can be kept in position by a combination of mooring lines and pontoons or with pontoons only. The most feasible alternative will depend on the site conditions such as span length, water depth, bottom conditions, ship traffic, environmental loading (waves, current, earthquake) etc.

A submerged floating tunnel can be an alternative crossing both to rock tunnels below the sea bottom and to long span bridges above the surface.



Compared with long span cable-stayed and suspension bridges, the increase of cost with span length is generally much better for the submerged floating tunnels. Rock tunnels will on the other hand increase in cost with depth to rock bottom (increasing the total length) and the rock conditions with respect to excavation costs.

This paper discusses stochastic dynamic response of a submerged floating tunnel subjected to wind driven waves and time domain earthquake analysis with particular emphasis on fluid structure interaction. Design analyses to check if specified safety criteria are met are not considered. The paper will discuss alternative numerical models and evaluate by comparing relative levels of selected response quantities. Some locations along the bridge will have three dimensional flow conditions. Typically this will be around pontoons and connections between the tunnel and the pontoons, and at the shore connections. In these areas a Navier-Stokes formulation for a finite element analysis of the fluid/structure interaction is expected to provide reference solutions that will contribute to obtain more economic structures to meet the target safety levels.

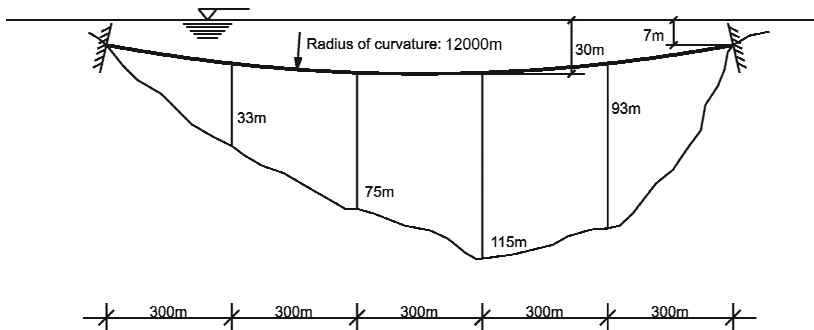


Figure 1: Submerged floating tunnel with tether mooring.

2 Dynamic response analyses

2.1 Dynamic equilibrium equation

When the structure is discretized by means of the finite element method the relationship between the loading and response stochastic processes is expressed as an equilibrium equation on matrix form. A fairly general expression in the time domain is given by:

$$\int_0^{+\infty} \mathbf{M}(t-\tau) \ddot{\mathbf{r}} d\tau + \int_0^{+\infty} \mathbf{C}(\mathbf{r}, \dot{\mathbf{r}}, t-\tau) \dot{\mathbf{r}} d\tau + \mathbf{K}(\mathbf{r}) \mathbf{r}(t) = \mathbf{Q}(t)$$

The lower integration limit is 0 due to the principle of causality. The convolution integrals are due to the mass and damping matrices being frequency dependent. Nonlinearities are accounted for by allowing the damping matrix to be a function of displacement and velocity, and the stiffness matrix a function of displacement. In addition to the equilibrium equation, initial displacement and velocity vectors

at time $t = 0$ must be specified. The mass matrix includes both structural and hydrodynamic contributions, with the latter being frequency dependent while the former generally is taken to be constant for submerged tunnels. Similarly, the damping matrix includes a frequency dependent hydrodynamic term and a constant structural contribution modelled e.g. by means of Rayleigh damping. Typically, the dependence on the displacement and velocity vector is neglected for the present type of structure. The structural stiffness matrix also includes contributions due to possible surface-piercing members such as pontoons in addition to tethers and anchor lines.

For the special case that the frequency dependence of the mass and damping matrices can be neglected, the two convolution integrals in the equilibrium equation disappear which results in a simple product form for the inertia and damping terms. For a stepwise time-integration of the system equations, it is furthermore convenient to express the equilibrium equation on incremental form.

2.2 Response analysis in the frequency domain

In the following, it is assumed that the structural matrices and the hydrodynamic loading have been linearized. From the theory of multi-degree-of-freedom systems under random loading, the response spectral density matrix can be expressed in terms of the load spectral matrix as:

$$\mathbf{S}_r(\omega) = \mathbf{H}(\omega)\mathbf{S}_Q\mathbf{H}^{*T}(\omega)$$

where

$$\mathbf{H}(\omega) = [\mathbf{K} + i\omega\mathbf{C}(\omega) - \omega^2\mathbf{M}(\omega)]^{-1}$$

is the *virtual frequency response function* of the structure-fluid system. In turn, the load matrix can be expressed by the one-dimensional sea elevation spectral density, yielding:

$$\mathbf{S}_r(\omega) = \mathbf{H}(\omega)\mathbf{F}(\omega)\mathbf{H}^{*T}(\omega)S_\eta(\omega) = \mathbf{B}(\omega)S_\eta(\omega)$$

where $\mathbf{F}(\omega)$ is referred to as the *hydrodynamic transfer function*. The matrix $\mathbf{B}(\omega)$ is designated the *transfer function* of the total system relating the response spectral density matrix to the scalar wave spectral density.

These two matrices also account for directionality effects related to hydrodynamic loading and structural response. In addition to the mean direction of the incoming wave system, the directional spreading of wave energy around this direction is important. This is expressed in terms of the wave spreading function $\Psi(\theta)$ where θ is the wave direction. The load amplitudes (per unit wave height) will typically also depend on the direction of the incoming wave. Furthermore, the structural response may exhibit a strong sensitivity to load direction.

By introducing the direction and frequency-dependent loading $\mathbf{Q}(\omega, \theta)$, the directional integration can be expressed on the following form:



$$\mathbf{F}(\omega) = \int_{\theta} \mathbf{Q}(\omega, \theta) \mathbf{Q}^{*T}(\omega, \theta) \Psi(\theta) d\theta$$

where the directional integration can be performed either on element or system level.

Accurate computation of the direction and frequency dependent load vector requires in general utilization of advanced and time-consuming numerical schemes such as the sink-and source method. The same applies to the frequency-dependent hydrodynamic contributions to the damping and mass matrices. In particular, submerged tunnels with complex geometries, caused e.g. by surface pontoons, demands careful modelling and fine-meshed spatial discretization if high precision is aimed at. However, at a preliminary design stage simplifications can be introduced in order to increase the computational efficiency. As an example, three-dimensional hydrodynamic models can be assembled from a sequence of two-dimensional approximations. Furthermore, analytical or semi-analytical expressions for axi-symmetric three-dimensional components such as pontoons and shafts can be utilized.

Due to the dynamic amplification effects, there will be a significant sensitivity of the response with respect to variation in peak period of the extreme sea state. Accordingly, a more consistent approach is to establish a so-called long-term statistical distribution. Probability distributions of local response maxima are then computed for a number of sea-states. The significant wave heights and peak periods are identified, together with corresponding frequencies of occurrence from the so-called scatter diagram applicable for the relevant bridge site. The long-term distribution of local response maxima is subsequently obtained as a weighted combination of the distributions for all these sea-states. The response level corresponding to a given return period is finally estimated by specifying the corresponding probability of exceeding maxima, and then inverting the long-term distribution.

A particular feature of some submerged tubular bridge concepts is a significant sensitivity of structural response to main wave direction and degree of directional spreading. This implies that the relative frequency of occurrence for a number of wave directions and corresponding spreading parameters must be considered when computing the long-term distribution.

2.3 Response analysis in the time domain

The time domain analysis is based on simulation of one or more samples of the stochastic load process. The samples can be generated for instance by means of Monte Carlo simulation methods, see e.g. [1,2,3]. For each of these sample functions, the corresponding load vector time series is computed, and subsequently a deterministic type of response analysis is performed.

In this type of approach, the sea-elevation process can be approximated by a discrete sum as:

$$\eta(\mathbf{x}, t) = \sum_{k=1}^{N_1} \sum_{l=1}^{N_2} A_{kl} \left\{ \cos \omega_k t - \kappa(\omega_k) \cdot (x \cos \theta_l + y \sin \theta_l) + \phi_{kl} \right\}$$



where

$$A_{kl} = \sqrt{2S_{\eta}(\omega_k, \theta_l) \Delta\omega \Delta\theta}$$

Here, ϕ_{kl} are random independent phase angles distributed uniformly between 0 and 2π . Furthermore,

$$\Delta\omega = \frac{\omega_{up}}{N_1} \quad \text{and} \quad \omega_k = (k-1)\Delta\omega$$

$$\Delta\theta = \frac{(\theta_{up} - \theta_{low})}{N_2} \quad \text{and} \quad \theta_l = \theta_{low} + (l-1)\Delta\theta$$

where ω_{up} is the upper limit of the frequencies to be included in the analysis; θ_{up} and θ_{low} designate the upper and lower limits for the summation with respect to wave direction.

The double summation can be efficiently carried out by means of FFT-techniques. Evaluation of the load vector for the submerged bridge can be performed based on the same type of expression simply by inserting the frequency and direction dependent (complex-valued) vector transfer functions between each harmonic component of the sea-elevation process and the corresponding harmonic load vector component, i.e.:

$$\mathbf{Q}(t) = \sum_{k=1}^{N_1} \sum_{l=1}^{N_2} A_{kl} \mathbf{Q}(\omega_k, \theta_l) \{ \cos \omega_k t - \kappa(\omega_k) \cdot (x \cos \theta_l + y \sin \theta_l) + \phi_{kl} \}$$

where for each component of the load vector a double summation of the same type as for the sea-elevation process is obtained.

For each generated sample of hydrodynamic load time series, corresponding response time series are computed by step by step time integration of the equations of motion.

2.4 Assessment of response analysis procedures in the frequency versus time domain

Summarizing the main features of the response analysis procedures, the benefits of the *frequency domain approach* are as follows:

- Frequency dependency of hydrodynamic coefficients for damping, added mass and excitation forces are easily incorporated
- Estimation of extreme values for design purposes is straightforward due to available closed-form analytical expressions
- The computational effort is significantly reduced as compared to time domain analysis.

However, on the negative side this type of analysis is not well-suited for incorporation of nonlinearities related to structural behaviour or hydrodynamic modelling. The benefits of the *time domain approach* can be summarized as:

- Nonlinear effects related e.g. to nonlinear material behaviour, geometric stiffness, finite surface wave effects and viscous loading can be incorporated in a direct manner



- Simulation in the time domain provides insight into the physical behaviour of the structure. Instantaneous deformation patterns and time variation of response can be easily visualized.

Among the negative aspects of this procedure are: Increased effort related to estimation of extreme response statistics, and difficulties related to implementation of frequency dependent damping and mass coefficients. Typically, both types of analyses should be performed in order to assess the importance of various modelling assumptions in relation to computed response.

3 Numerical studies

3.1 Global response from wind generated waves

Loading due to wind generated waves is a major load case for the assessment of dynamic response properties for a submerged floating tunnel. The following numerical studies will focus on the effect of spatial variation of the loading as mean wave direction and wave spreading.

3.1.1 Directionality effects for straight and horizontally curved bridge

The straight bridge is chosen for illustration of the principal effect. Similar effects are then illustrated for curved bridges which may represent the most likely geometry.

The response analyses are performed in the frequency domain with the computer program FEDAF [4]. The hydrodynamic loading and fluid interaction is calculated on the basis of linear potential theory. The JONSWAP [5] model spectrum has been used for the sea elevation. The directional spreading of wave energy is modelled by a frequency independent cosine function.

Two natural modes of vibration in the vertical direction for the straight bridge have natural frequencies $\omega_7 = 1.11 \text{ rad/s}$ and $\omega_8 = 1.29 \text{ rad/s}$. We apply long crested wave loading represented by an elevation spectrum with peak circular frequency $\omega_p = 0.4\pi (1.26 \text{ rad/s}, T_p = 5 \text{ s})$. With frequency ratios $\beta_7 = 1.135$ and $\beta_8 = 0.98$, significant dynamic amplification should be expected for these modes.

The degree of dynamic amplification is, however, also associated with the spatial load variation along the bridge in relation to the mode shapes. Maximum spatial amplification is obtained when the wavelength of a natural mode coincides with the wavelength of the incoming wave decomposed onto the bridge axis. This is illustrated in Fig. 2.

Cross sections of the bridge at a distance L_θ apart will be in phase with respect to hydrodynamic force. In order to obtain maximum dynamic amplification in mode 8 the value of L_θ should be 480 m, corresponding to $\theta = 4.67^\circ$ for a wave length $\lambda_p = 39 \text{ m} (\omega_p = 0.4\pi)$. For mode 7 the corresponding L_θ is 700 m and $\theta = 3.2^\circ$. Around $\theta = 4^\circ$ we should then expect



to get considerable dynamic amplification from both modes 7 and 8. This is verified by numerical calculations. Results in terms of maximum bending moment response along the bridge for a given θ are shown in Fig. 3.

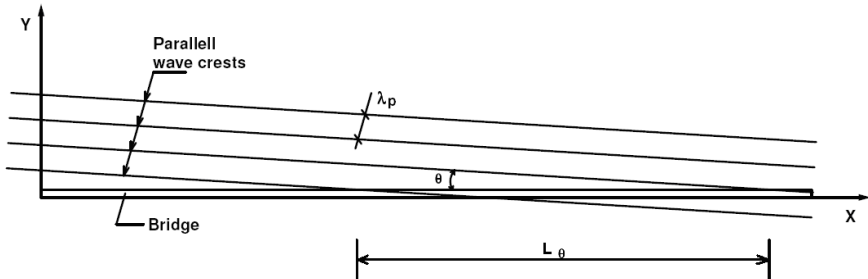


Figure 2: Parallel wave crests propagating towards the bridge at an angle θ from the bridge normal.

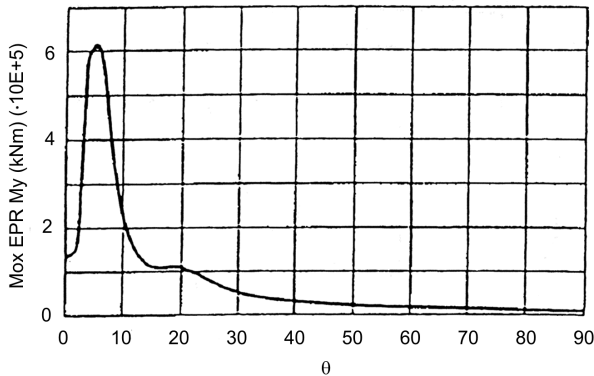


Figure 3: Maximum expectation value of bending moment in vertical bridge motion as function of mean wave direction.

If we look at the distribution of expected bending moment peak response along the bridge we can clearly identify from Fig. 4 the change from the symmetric low level response at $\theta = 0^\circ$ towards a much higher level and asymmetric response at $\theta = 5^\circ$. The shape of the curve for the latter angle of incidence is also identified as a combination of modes 7 and 8.

Some amplification of modes 7 and 8 can be expected also for angles of incidence corresponding to values of L_θ equal to $\frac{1}{2}, \frac{1}{4}, \frac{1}{6}$ and so on, especially if the possibility of interaction exists as for $\theta \approx 4^\circ$. In Fig. 3 we observe also a distinct peak for $\theta \approx 20^\circ$. The response distribution along the bridge has then a form similar to that for $\theta \approx 4^\circ$. The value of L_θ is now $\frac{1}{4}$ for mode 8 and $\frac{1}{6}$ for mode 7.

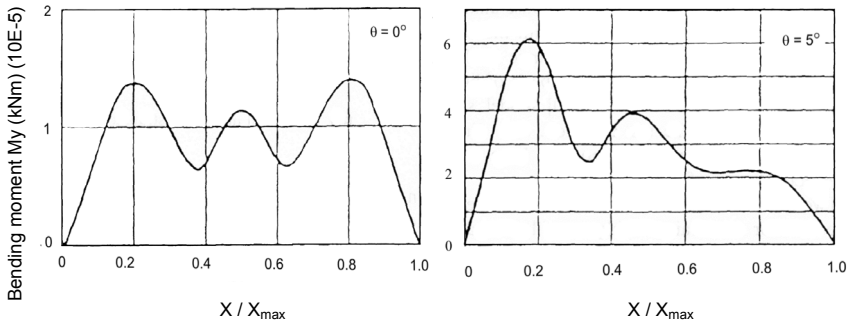


Figure 4: Expected peak response along the bridge for different wave propagation directions.

For a bridge that is curved with a curvature equal to 2000 m in the horizontal plane and with the same distance between the end points, the maximum bending moments in the vertical plane as function of the wave propagation angle is shown in Fig. 5. It is seen that we get significant effects from wave direction in the vicinity of the normal direction. The maximum bending moment is, however, lower for this case than for the straight bridge.

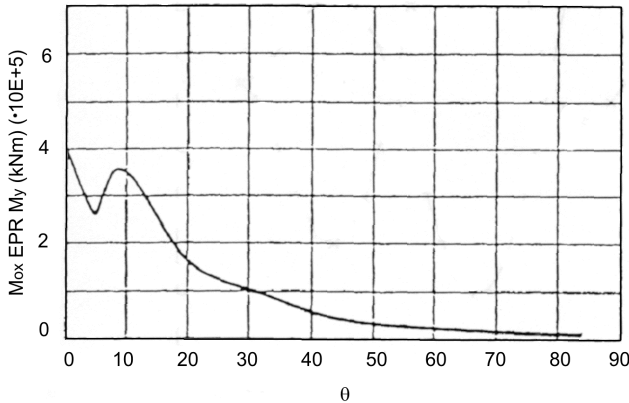


Figure 5: Maximum expectation value of bending moment about horizontal axis versus wave direction.

For $\theta = 0^\circ$ the bending moment response for the curved bridge is three times that of the straight bridge for normal wave incidence direction. This is largely contributed by a combined vertical/horizontal symmetric mode shape with a frequency ratio of 0.9.

3.1.2 Effects of wave direction and short crested wave load modelling

These effects are studied for the bridge in Fig. 1 without curvature in the horizontal direction. The net buoyancy of the tunnel is approximately 10% of the submerged weight. The analyses are performed in the frequency domain.



Short crested waves are defined with an energy spreading function $\Psi(\theta) = C \cdot \cos^8 \theta$ where θ is defined in the range $\pm \frac{\pi}{2}$. C is determined from the requirement of energy preservation. With a mean wave direction normal to vertical plane of the submerged tunnel, the maximum expected peak response away from the fixed ends of the tunnel has dropped to $0.65 \cdot 10^6$ kNm compared with $1.85 \cdot 10^6$ kNm for long crested waves. Short crested waves with a mean direction of 1° from the normal will give a maximum response equal to $0.57 \cdot 10^6$ kNm as compared with $0.50 \cdot 10^6$ kNm for long crested waves.

For a vertically curved submerged floating tunnel, the present study has demonstrated high sensitivity of bending moment response to directionally for long crested waves. Response analyses for design purposes will have to consider a range of variation of the peak load period T_p of the sea elevation spectrum. This is order to find the maxima associated with close natural periods and to excitation from consecutive waves of varying non-normal incidence.

For short crested waves there is a general reduction in response for this bridge and the directional sensitivity is not pronounced. In cases of counteracting directionality effects for long crested waves as for the 1° case above, the response may become higher for a short crested wave load model. An economical and still safe design will require reliable information about the actual wave spreading for the actual site of the submerged floating tunnel.

3.2 Response to earthquake excitation

A major purpose with the earthquake analyses is to show the relative difference in response results for models with and without fluid element modelling for the fluid structure interaction when vertical waves are propagating through the water.

The finite element model applied for the earthquake response analyses is illustrated in Fig. 6. It has been established in the computer program ABAQUS [6]. The bridge is modelled by thin shell elements and the tethers by cable elements. The buoyancy excess for the tunnel will provide sufficient pretension to prevent the cables from becoming slack. The 3D elements of the fluid are so-called acoustic elements. The vertical ground motion in terms of the acceleration history is transferred through the shore connections at both ends of the bridge, the four mooring tendons and the fluid surrounding the bridge shell model. The bridge is curved both in the vertical and horizontal directions with curvatures $R_{vertical} = 12000\text{ m}$ and $R_{horizontal} = 2000\text{ m}$.

The Nahanni earthquake (Canada 1985) is selected for the earthquake excitation. This choice is rather arbitrary, but this earthquake will fit the Norwegian design spectrum well. The three orthogonal components are applied simultaneously. Phase delay is introduced along the axis through the end points of the bridge. The vertical component of the recorded ground acceleration is



shown in Fig 7. The numerical model is linear in the sense that the magnitude of the response quantities will scale proportionally with the ground excitation.

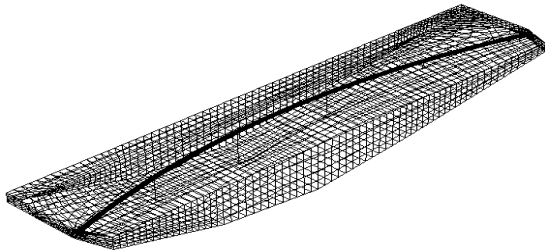


Figure 6: Integrated finite element model with bridge and surrounding fluid.

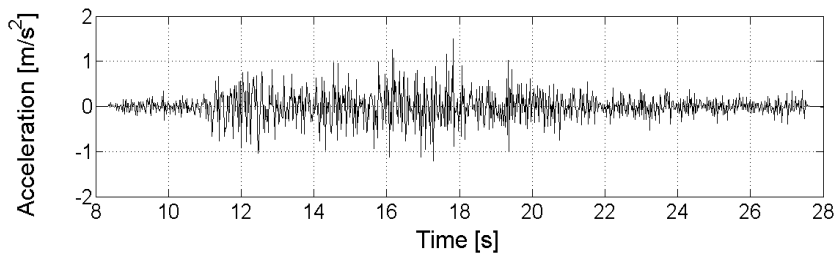


Figure 7: Vertical acceleration component of the Nahanni earthquake (Canada 1985).

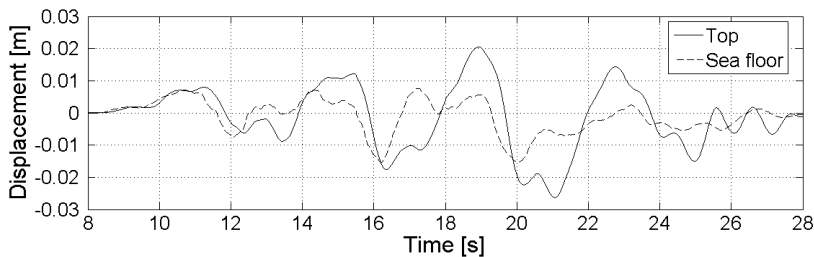


Figure 8: Vertical motion at the top of the tether and at the anchoring foundation.

The response time series in Fig. 8 show the vertical displacement of the two end points of tether number 3 from the left shore. The solid line gives the vertical motion at the tunnel, while the dashed line defines the input motion to the anchoring foundation from the soil motion. Both time series are computed from the integrated model with fluid elements. Figure 9 compare the vertical motion at the same location on the tunnel as in Fig. 8. Again the solid line shows results from the integrated fluid structure model, while the dashed line is computed with a model with the fluid represented only as added mass. The added mass



coefficients vary along the bridge as distance to bottom and surface varies from the central parts and towards the ends [7]. We can notice that the maximum amplitude values are fairly close for the two models. There is an increase in double amplitude of approximately 10%. We also notice that there is a phase delay between the two response time series. This is not important for design purposes, but could be expected both from differences in wave propagation velocity through the tendons and through the water and from the sloping bottom towards the shores. This will influence both wave travelling distance and normal direction.

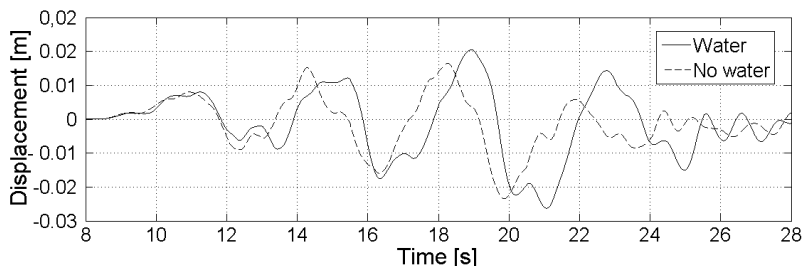


Figure 9: Vertical motion at the top of the tether shown for the fluid structure interaction model as well as for the simplified fluid structural model.

References

- [1] Borgman, L.E.: "Ocean Wave Simulation for Engineering Design", *Journal of Waterways and Harbours Division*, ASCE, Vol.95, No.WW4, 1969, pp 556-583.
- [2] Shinozuka, M.: "Monte Carlo Solution of Structural Dynamics", *Computers and Structures*, Vol. 2, 1972, pp 855.
- [3] Hammersley, F. and Handscomb, P.: "*Monte Carlo Methods*", Methuen, London, 1964.
- [4] FEDAF, Dynamic analysis of floating and submerged tubular bridges, User's Manual, SINTEF-report STF71 F88022, Trondheim 1989.
- [5] Hasselmann K, et al. Measurements of wind-wave growth and swell decay during the joint North Sea wave project (JONSWAP). *Ergänzungsheft zur Deutschen Hydrographischen Zeitschrift*, A No12, 1973.
- [6] ABAQUS Standard version 6.4, ABAQUS Inc 2004.
- [7] Greenhow M. Hydrodynamic loading on horizontal cylinders. Unpublished project memo, Marintek, Trondheim, 1988.